

Probing Majorana fermions in spin-orbit coupled atomic Fermi gases

Xia-Ji Liu¹, Lei Jiang², Han Pu², and Hui Hu¹

¹*ACQAO and Centre for Atom Optics and Ultrafast Spectroscopy,
Swinburne University of Technology, Melbourne 3122, Australia*

²*Department of Physics and Astronomy, and Rice Quantum Institute, Rice University, Houston, TX 77251, USA*

(Dated: May 23, 2022)

We examine theoretically the visualization of Majorana fermions in a two-dimensional trapped ultracold atomic Fermi gas with spin-orbit coupling. By increasing an external Zeeman field, the trapped gas transits from non-topological to topological superfluid, via a mixed phase in which both types of superfluids coexist. We show that the zero-energy Majorana fermion, supported by the topological superfluid and localized at the vortex core, may be visible through (i) the core density and (ii) the local density of states, which are readily measurable in experiment. We present a realistic estimate on experimental parameters for ultracold ⁴⁰K atoms.

PACS numbers: 05.30.Jp, 03.75.Mn, 67.85.Fg, 67.85.Jk

Majorana fermion [1] - particle that is its own antiparticle - has attracted considerable attentions from a wide area of physics [2]. A particular interest comes from its non-Abelian exchange statistics that is crucial for topological quantum computation [3, 4]. Two well separated Majorana fermions may form a non-local fermionic state, as a non-local qubit for inherently fault-tolerant quantum memory. As a portal for future quantum technology, the realization of Majorana fermions in a highly controllable manner is of great importance and a timely quest.

Majorana fermions are believed to exist in a number of two-dimensional (2D) physical settings, including fractional quantum Hall states at filling $\nu = 5/2$ [5], vortex states of $p_x + ip_y$ superconductors/superfluids [6, 7], and surfaces of 3D topological insulators in proximity to a s -wave superconductor [8]. Majorana fermions may also emerge in 1D quantum systems with strong spin-orbit coupling, such as quantum wires [9] and optically trapped 1D fermionic atoms [10]. All these appealing proposals are yet to be realized experimentally.

In this work, we examine the possibility of observing Majorana fermions in the vortex core of a spin-orbit coupled ultracold atomic Fermi gas in 2D harmonic traps. This is a scenario discussed earlier by several researchers [11–13], based on a theoretical concept originated from Jackiw and Rossi, who predicted the existence of vortex-core Majorana fermions in (2+1) dimensional Dirac theory [14]. Here, we perform a fully microscopic calculation with Bogoliubov-de Gennes (BdG) equation, which enables simulations with realistic experimental parameters. Our study is motivated by the recent creation of non-Abelian gauge fields in a Bose-Einstein condensate (BEC) of ⁸⁷Rb atoms [15] and its possible realization in fermionic ⁴⁰K atoms [16].

We find that by increasing a Zeeman field, a topological superfluid emerges from the trap edge and extends gradually to the whole Fermi cloud, supporting zero-energy states (ZES) at the vortex core and trap edge. This topological phase transition is detectable through a sudden change of the atomic density inside the vortex core, associated with the occupation of the Majorana state. We

show that the wave function of the Majorana fermions can be inferred from the local density of states (LDOS) at the core.

Mean-field BdG equation. — We consider a trapped 2D atomic Fermi gas subject to Rashba spin-orbit coupling $V_{\text{SO}}(\mathbf{r}) = -i\lambda(\partial_y + i\partial_x)$ and a Zeeman field h , which may be prepared in a single pancake-like optical trap $V(\mathbf{r}, z) = M[\omega_{\perp}^2 r^2 + \omega_z^2 z^2]/2$ with trapping frequencies $\omega_z \gg \omega_{\perp}$. We note that 2D Fermi gas has recently been realized in experiments [17, 18]. The system is described by $\mathcal{H} = \int d\mathbf{r} [\mathcal{H}_0(\mathbf{r}) + \mathcal{H}_I(\mathbf{r})]$, where

$$\mathcal{H}_0(\mathbf{r}) = \sum_{\sigma=\uparrow,\downarrow} \psi_{\sigma}^{\dagger} \mathcal{H}_{\sigma}^S(\mathbf{r}) \psi_{\sigma} + [\psi_{\uparrow}^{\dagger} V_{\text{SO}}(\mathbf{r}) \psi_{\downarrow} + \text{H.c.}] \quad (1)$$

and $\mathcal{H}_I(\mathbf{r}) = U_0 \psi_{\uparrow}^{\dagger}(\mathbf{r}) \psi_{\downarrow}^{\dagger}(\mathbf{r}) \psi_{\downarrow}(\mathbf{r}) \psi_{\uparrow}(\mathbf{r})$ describes the contact interaction between opposite spins. Here $\psi_{\uparrow,\downarrow}^{\dagger}$ are the creation field operators for the spin-up and -down atoms, $\mathcal{H}_{\sigma}^S = -\hbar^2 \nabla^2 / (2M) + M\omega_{\perp}^2 r^2 / 2 - \mu - h\sigma_z$ is the single-particle Hamiltonian in reference to the chemical potential μ . The interaction strength U_0 is to be regularized via $1/U_0 + \sum_{\mathbf{k}} 1/(\hbar^2 \mathbf{k}^2 / M + E_a) = M/(4\pi\hbar^2) \ln(E_a/E)$. Here E_a is the binding energy of the two-body bound state [19, 20] and $E > 0$ is the relative collision energy.

The low-energy fermionic quasiparticles are solved by the mean-field BdG approach, $\mathcal{H}_{\text{BdG}} \Psi_{\eta}(\mathbf{r}) = E_{\eta} \Psi_{\eta}(\mathbf{r})$. Using the convention for Nambu spinors $\Psi_{\eta}(\mathbf{r}) = [u_{\uparrow\eta}, u_{\downarrow\eta}, v_{\uparrow\eta}, v_{\downarrow\eta}]^T$, the BdG Hamiltonian reads,

$$\mathcal{H}_{\text{BdG}} = \begin{bmatrix} \mathcal{H}_{\uparrow}^S(\mathbf{r}) & V_{\text{SO}}(\mathbf{r}) & 0 & -\Delta(\mathbf{r}) \\ V_{\text{SO}}^{\dagger}(\mathbf{r}) & \mathcal{H}_{\downarrow}^S(\mathbf{r}) & \Delta(\mathbf{r}) & 0 \\ 0 & \Delta^*(\mathbf{r}) & -\mathcal{H}_{\uparrow}^S(\mathbf{r}) & V_{\text{SO}}^{\dagger}(\mathbf{r}) \\ -\Delta^*(\mathbf{r}) & 0 & V_{\text{SO}}(\mathbf{r}) & -\mathcal{H}_{\downarrow}^S(\mathbf{r}) \end{bmatrix}, \quad (2)$$

where $\Delta = -(U_0/2) \sum_{\eta} [u_{\uparrow\eta} v_{\downarrow\eta}^* f(E_{\eta}) + u_{\downarrow\eta} v_{\uparrow\eta}^* f(-E_{\eta})]$ is the order parameter, to be solved self-consistently in conjunction with the atomic densities, $n_{\sigma}(\mathbf{r}) = (1/2) \sum_{\eta} [|u_{\sigma\eta}|^2 f(E_{\eta}) + |v_{\sigma\eta}|^2 f(-E_{\eta})]$. Here $f(x) \equiv 1/(e^{x/k_B T} + 1)$ is the Fermi distribution function. The chemical potential μ is determined by the total atom number $N = \int d\mathbf{r} [n_{\uparrow}(\mathbf{r}) + n_{\downarrow}(\mathbf{r})]$. With

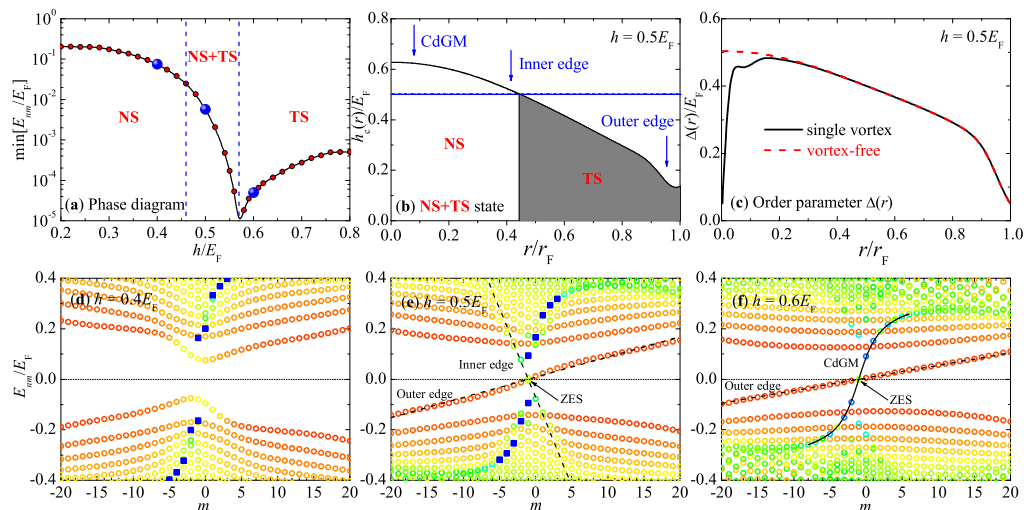


Figure 1: (color online) (a) Phase diagram, along with the lowest eigenenergy of Bogoliubov spectrum. (b) Configuration of the mixed phase at $h = 0.5E_F$. The local critical field is calculated in the vortex-free state. (c) The gap profile with and without vortex at $h = 0.5E_F$. (d), (e), and (f) Energy spectrum at $h/E_F = 0.4, 0.5$, and 0.6 (where $E_F = \hbar^2 k_F^2 / (2M) = \sqrt{N} \hbar \omega_\perp$ is the Fermi energy) in the presence of a single vortex. The color of symbols indicates the mean radius $\sqrt{\langle r^2 \rangle} / r_F$ (where $r_F = (4N)^{1/4} \sqrt{\hbar / (M \omega_\perp)}$ is the Fermi radius) of the eigenstate, which is defined by $\langle r^2 \rangle = \int r^2 [|u_\uparrow|^2 + |u_\downarrow|^2 + |v_\uparrow|^2 + |v_\downarrow|^2] dr$. The color of symbols changes from blue when the excited state is localized at the trap center to red when its mean radius approaches the Thomas-Fermi radius. The CdGM states are indicated by blue squares in (d) and (e), and by a solid line in (f). The dashed lines show the inner edge and outer edge branches.

a single vortex at trap center, we take $\Delta(\mathbf{r}) = \Delta(r)e^{-i\varphi}$ and decouple the BdG equation into different angular momentum channels indexed by an integer m . The quasiparticle wave functions take the form, $[u_\uparrow(r)e^{-i\varphi}, u_\downarrow(r), v_\uparrow(r)e^{i\varphi}, v_\downarrow(r)]e^{i(m+1)\varphi} / \sqrt{2\pi}$. We have solved self-consistently the BdG equations using the basis expansion method. For the results presented here, we have taken $N = 400$ and $T = 0$. We have used $E_a = 0.2E_F$ and $\lambda k_F / E_F = 1$, which are typical parameters that can be readily realized in a 2D ^{40}K Fermi gas [18]. Other sets of parameters, with varying interaction strength, SO coupling strength and temperature, have also been tried.

The use of Nambu spinor representation leads to an inherent redundancy built into the BdG Hamiltonian. \mathcal{H}_{BdG} is invariant under the *particle-hole* transformation, $u_\sigma(\mathbf{r}) \rightarrow v_\sigma^*(\mathbf{r})$ and $E_\eta \rightarrow -E_\eta$. Thus, every eigenstate with energy E has a partner at $-E$. These two states describe the same physical degrees of freedom, as the Bogoliubov quasiparticle operators associated with them satisfy $\Gamma_E = \Gamma_{-E}^\dagger$. In the expressions for order parameter and atomic density, this redundancy has been removed by multiplying a factor of $1/2$.

Majorana fermions. — The particle-hole redundancy, however, is very useful to illustrate a non-trivial feature when the Zeeman field h is beyond a threshold, $h > h_c = \sqrt{\mu^2 + \Delta^2}$ and the system is in a topological state [8], hosting ZES within the energy gap. Due to $E = 0$, the associated quasiparticle operators satisfy $\Gamma_0 = \Gamma_0^\dagger$. Thus, a zero-energy quasiparticle is its own

antiparticle - exactly the defining feature of a Majorana fermion [2]. Because of the redundant particle-hole representation, the ZES or Majorana fermion is a *half* of ordinary fermion and thus must always come in pairs. Each of the paired states, localized *separately* in real space, can hardly be pushed away from $E = 0$ by a local perturbation [4, 6], giving rise to the intrinsic topological stability enjoyed by Majorana fermions. It is straightforward to show from the BdG Hamiltonian that the wave function of Majorana fermions should satisfy either $u_\sigma(\mathbf{r}) = v_\sigma^*(\mathbf{r})$ or $u_\sigma(\mathbf{r}) = -v_\sigma^*(\mathbf{r})$. The former follows directly from the particle-hole symmetry. For the latter, the related quasiparticle operator satisfies $\tilde{\Gamma}_0 = -\tilde{\Gamma}_0^\dagger$. This is necessary for expressing an ordinary fermion using paired Majorana fermions [21].

Phase diagram. — Figure 1 reports the phase diagram (a) along with the quasiparticle energy spectrum of different phases (d, e, and f) in the presence of a single vortex. By increasing the Zeeman field, the system evolves from a non-topological state (NS) to a topological state (TS), through an intermediate mixed phase in which NS and TS coexist. The mixed phase, unique for a trapped system, can be easily understood from the point of view of local density approximation, in which the local chemical potential $\mu(\mathbf{r}) = \mu - M\omega_\perp^2 r^2 / 2$ and the order parameter $\Delta(\mathbf{r})$ decrease continuously away from the trap center. As a result, the local critical Zeeman field $h_c(\mathbf{r}) = \sqrt{\mu^2(\mathbf{r}) + \Delta^2(\mathbf{r})}$ becomes smaller at the trap edge, as shown in Fig. (1b) for $h = 0.5E_F$. This creates a ring of TS at the outer region where $h > h_c(\mathbf{r})$, surrounding the inner region which is non-topological.

The full topological transition occurs when the Zeeman field is larger than the critical field at the trap center, $h > \sqrt{\mu^2 + \Delta^2(0)}$, where $\Delta(0)$ is the gap at trap center in the absence of the vortex.

The topological phase transition into TS is well characterized by the low-lying quasiparticle spectrum, which has the particle-hole symmetry $E_{m+1} = -E_{-(m+1)}$. As shown in Fig. (1d), the spectrum of the NS is gapped by order parameter, even at the trap edge. In the mixed phase (Fig. (1e)), however, three branches with small energy spacing appear. The branches labeled as ‘‘Outer edge’’ and ‘‘Inner edge’’ consist of the eigenstates with wave functions localized at the edges of the TS as Andreev bound states, as indicated by the arrows in Fig. (1b). The two edge states at $m = -1$ have nearly zero energy. The other branch, shown by blue squares, is a series of discrete localized states at the vortex core, i.e., the so-called Caroli-de Gennes-Matricon (CdGM) states [22]. When the TS extends over the whole cloud (Fig. (1f)), the dispersion of the inner edge branch moves into the continuum. The energy of the state with $m = -1$ in both the CdGM branch and outer edge branch becomes essentially zero.

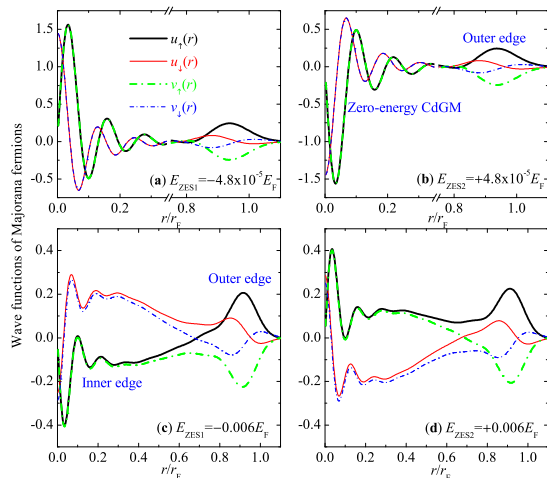


Figure 2: (color online) Wave functions of the two lowest-energy modes in the full topological state at $h = 0.6E_F$, (a) and (b), and in the partial topological state at $h = 0.5E_F$, (c) and (d). The wave functions are in units of $\sqrt{M\omega_\perp/\hbar}$.

The eigenstates with nearly zero energy at $m = -1$, i.e., the two edge states in the mixed phase as well as the outer edge state and CdGM state in the full TS, can be identified as zero-energy Majorana fermions in the thermodynamic limit. To show this, we plot in Fig. 2 the wave function of these eigenstates in the full TS (a and b) and in the mixed phase (c and d). In both cases, we observe a bond and anti-bond hybridization between two well-localized wave functions: one satisfies $u_\sigma(\mathbf{r}) = v_\sigma^*(\mathbf{r})$ and the other $u_\sigma(\mathbf{r}) = -v_\sigma^*(\mathbf{r})$, which is exactly the symmetry of the wave function required by Majorana fermions. The hybridization is caused by a quasiparticle tunneling between paired Majorana states [23], which

leads to the splitting of degenerate zero-energy states to finite energies $\pm E_{\text{ZES}}$. The tunneling barrier between the two edge states is lower, so the energy splitting is relatively larger (i.e., $E_{\text{ZES}} \approx 0.006E_F$). In contrast, the tunneling between the outer edge state and CdGM state seems to be more difficult, giving rise to an exponentially small splitting (i.e., $E_{\text{ZES}} \approx 4.8 \times 10^{-5}E_F$).

The different phases can therefore be identified from the lowest eigenenergy of energy spectrum, as plotted in Fig. (1a). Within the NS, it decreases slowly as the Zeeman field increases. The decrease becomes exponentially fast with the appearance of a partial TS and a minimum is reached when the cloud just becomes fully TS. Further increase of the Zeeman field will reduce the order parameter and hence the tunneling barrier between the two Majorana states, which are localized respectively at the vortex core and trap edge, leading to a steady increase of the lowest eigenenergy. We note that the exponentially small energy of Majorana fermions in the full TS, inherent to the finiteness of trapped Fermi cloud, should be suppressed by increasing the number of total atoms.

Probing Majorana fermions. — In the TS, the occupation of the Majorana vortex-core state affects significantly the atomic density and LDOS of the Fermi cloud near the trap center, which in turn gives an unambiguous experimental signature for observing Majorana fermions.

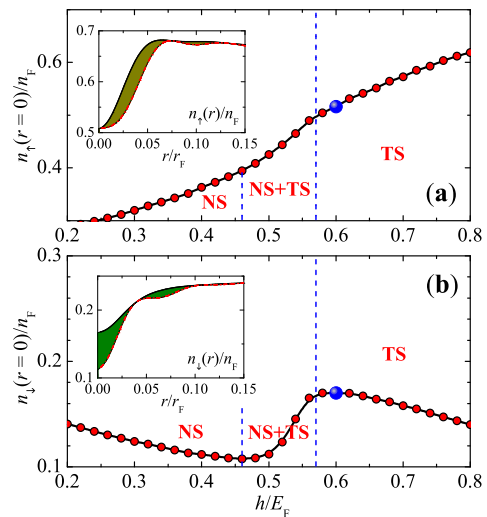


Figure 3: (color online) Zeeman field dependence of spin-up (a) and spin-down (b) densities at the vortex core. The density is normalized by the Thomas-Fermi density $n_F = (\sqrt{N}/\pi)\sqrt{M\omega_\perp/\hbar}$. The insets show the core density distributions at $h = 0.6E_F$. The red dot-dashed lines show the result by excluding artificially the Majorana vortex core state, whose contribution is shown by the shaded area.

Figure 3 presents the spin-up and -down densities at the trap center, $n_\uparrow(0)$ and $n_\downarrow(0)$, as a function of the Zeeman field. In general, $n_\uparrow(0)$ and $n_\downarrow(0)$ increases and decreases respectively with increasing field. However, we find a sharp increase of $n_\downarrow(0)$ when the system evolves from the mixed phase to the full TS. Accordingly, a

change of slope or kink appears in $n_{\uparrow}(0)$. The increase of $n_{\downarrow}(0)$ is associated with the *gradual* formation of the Majorana vortex-core mode, whose occupation contributes notably to atomic density due to the *large* amplitude of its localized wave function. We plot in the inset of Fig. (3b) $n_{\downarrow}(0)$ at $h = 0.6E_F$, with or without the contribution of the Majorana mode, which is highlighted by the shaded area. This contribution is apparently absent in the NS. Thus, a sharp increase of $n_{\downarrow}(0)$, detectable in in-situ absorption imaging, signals the topological phase transition and the appearance of the Majorana vortex-core mode. This feature persists at typical experimental temperature, i.e., $T = 0.1T_F$. We note that experimentally it is more favorable to take a time-of-flight imaging of the cloud after an expansion time, in order to have enough resolution to visualize the vortex core. We anticipate the sharp increase in $n_{\downarrow}(0)$ may persist for a short expansion time. Alternatively, we may tune quickly an external magnetic field to take the Fermi system to the BEC limit across Feshbach resonances. In this way, the vortex core can be imaged clearly after the time-of-flight just like in an atomic BEC.

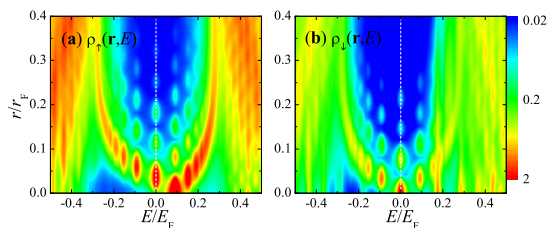


Figure 4: (color online) Log-scale contour plot of the LDOS for spin-up (a) and spin-down (b) atoms at $h = 0.6E_F$. Here we use $\Gamma = 0.01E_F$. The LDOS is units of n_F/E_F .

In the full TS, the wave function of the Majorana mode can be determined by measuring LDOS through

spatially resolved rf-spectroscopy [24, 25], which provides a cold-atom analog of the widely used scanning tunneling microscope in solid state. We show in Fig. 4 the spin-up and -down LDOS at $h = 0.6E_F$ defined as $\rho_{\sigma}(\mathbf{r}, E) = (1/2) \sum_{\eta} [|u_{\sigma\eta}|^2 \delta(E - E_{\eta}) + |v_{\sigma\eta}|^2 \delta(E + E_{\eta})]$, where the δ -function can be simulated by a Lorentzian distribution with a suitable energy broadening Γ . Inside the vortex core, the contribution from the Majorana mode and other CdGM states is clearly visible within the superfluid gap. In the case of $\Gamma, k_B T < \Delta E$, where $\Delta E \sim \Delta^2(0)/(2E_F)$ is the energy spacing of CdGM states [22] which for typical parameters as used in our calculation turns out to be about 10 nK, the Majorana fermion contribution $\rho_{\sigma, \text{ZES}}(\mathbf{r}, 0)$ may be singled out. As $\rho_{\sigma, \text{ZES}}(\mathbf{r}, 0) \propto |u_{\sigma\eta}(\mathbf{r})|^2 = |v_{\sigma\eta}(\mathbf{r})|^2$, the spatially resolved rf-spectroscopy maps out directly the wave function of the Majorana vortex-core state.

In closing, we note that 2D ultracold atomic Fermi gases are an ideal platform for probing and manipulating Majorana fermions because of the unprecedented controllability and flexibility. This is particularly useful for the purpose of topological quantum computation, using Majorana fermions as qubits [4]. For instance, two 2D atomic Fermi gases formed by a double-well potential along z -axis, each of which has a single vortex at the center, can host four Majorana fermions for carrying out the basic information process. In this configuration, inter-well quantum tunneling of Majorana fermions is possible, providing another potential means to detect the interesting topological phase transition.

Acknowledgment — We thank Peter Drummond, Chris Vale, and Peter Hannaford for helpful discussions. HH and XJL are supported by the ARC Discovery Project (Grant No. DP0984522 and DP0984637) and NFRP-China (Grant No. 2011CB921502). HP is supported by the NSF and the Welch Foundation (Grant No. C-1669).

-
- [1] E. Majorana, *Nuovo Cimentto* **14**, 171 (1937).
[2] F. Wilczek, *Nature Phys.* **5**, 614 (2009).
[3] A. Kitaev, *Ann. Phys. (N.Y.)* **321**, 2 (2006).
[4] C. Nayak *et al.*, *Rev. Mod. Phys.* **80**, 1083 (2008).
[5] G. Moore and N. Read, *Nucl. Phys.* **B360**, 362 (1991).
[6] N. Read and D. Green, *Phys. Rev. B* **61**, 10267 (2000).
[7] T. Mizushima, M. Ichioka, and K. Machida, *Phys. Rev. Lett.* **101**, 150409 (2008).
[8] L. Fu and C. L. Kane, *Phys. Rev. Lett.* **100**, 096407 (2008); J.D. Sau *et al.*, *Phys. Rev. Lett.* **104**, 040502 (2010); J. Alicea, *Phys. Rev. B* **81**, 125318 (2010); L. Mao and C. Zhang, *Phys. Rev. B* **82**, 174506 (2010); P. Hosur *et al.*, *Phys. Rev. Lett.* **107**, 097001 (2011).
[9] R. M. Lutchyn, J. D. Sau, and S. D. Sarma, *Phys. Rev. Lett.* **105**, 077001 (2010); Y. Oreg, G. Refael, and F. von Oppen, *Phys. Rev. Lett.* **105**, 177002 (2010); J. Alicea *et al.*, *Nature Phys.* **7**, 412 (2011).
[10] L. Jiang *et al.*, *Phys. Rev. Lett.* **106**, 220402 (2011).
[11] C. Zhang *et al.*, *Phys. Rev. Lett.* **101**, 160401 (2008).
[12] M. Sato, Y. Takahashi, and S. Fujimoto, *Phys. Rev. Lett.* **103**, 020401 (2009).
[13] S.-L. Zhu *et al.*, *Phys. Rev. Lett.* **106**, 100404 (2011).
[14] R. Jackiw and P. Rossi, *Nucl. Phys. B* **190**, 681 (1981).
[15] Y.-J. Lin, K. Jiménez-García, and I. B. Spielman, *Nature (London)* **471**, 83 (2011).
[16] J.D. Sau *et al.*, *Phys. Rev. B* **83**, 140510(R) (2011).
[17] P. Dyke *et al.*, *Phys. Rev. Lett.* **106**, 105304 (2011).
[18] B. Fröhlich *et al.*, *Phys. Rev. Lett.* **106**, 105301 (2011).
[19] M. Randeria, J.-M. Duan, and L.-Y. Shieh, *Phys. Rev. Lett.* **62**, 981 (1989).
[20] D. S. Petrov, M. A. Baranov, and G. V. Shlyapnikov, *Phys. Rev. A* **67**, 031601(R) (2003).
[21] The ordinary fermion operator at $E = 0$ is given by $c = \Gamma_0 + \tilde{\Gamma}_0$. By defining Majorana operators $\gamma_1 = \Gamma_0$ and $\gamma_2 = i\tilde{\Gamma}_0$, we express $c = \gamma_1 - i\gamma_2$, as anticipated.
[22] C. Caroli, P. G. de Gennes, and J. Matricon, *Phys. Lett.* **9**, 307 (1964).
[23] T. Mizushima, K. Machida, *Phys. Rev. A* **81**, 053605

- (2010).
- [24] Y. Shin *et al.*, Phys. Rev. Lett. **99**, 090403 (2007).
- [25] L. Jiang *et al.*, Phys. Rev. A **83**, 061604(R) (2011).